JOURNAL OF APPLIED ELECTROCHEMISTRY 19 (1989) 368–376

Active–passive behaviour and stress corrosion cracking of A516 steel in Bayer solution

HUY HA LE, EDWARD GHALI

Department of Mining and Metallurgy, Laval University, Quebec, Canada G1K 7P4

Received 23 May 1988; revised 23 November 1988

The susceptibility of A516 steel to stress corrosion cracking (SCC) is essentially restricted to the active–passive range and it increases with the presence of AlO_2^- ions or other impurities of Bayer solution in the electrolytes. The application of anodic protection for preventing SCC does not completely eliminate the danger of cracking, particularly in caustic aluminate and Bayer solutions. The formation of an Fe_3O_4 layer in the active–passive zone and Fe_2O_3 in the passive zone is very likely. In the presence of AlO_2^- ions, an amorphous film of $Fe_{3-x}Al_xO_4$ ($x \leqslant 2$) is observed on the electrode surface and leads very probably to an increased susceptibility to embrittlement. The corrosion behavior diagram (CBD) method, as well as the critical and passive current densities, the corrosion rates and the activation energy support strongly that passivation is easier, but less protective, against SCC in the presence of AlO_2^- ions and impurities in Bayer solution than in pure NaOH. The calculated activation energy suggests that the mechanism of dissolution-controlled cracking is the principal process in SCC of A516 in these studied solutions.

1. Introduction

It has been recognized that stress corrosion cracking (SCC) of carbon steel in hot caustic solutions is a dangerous phenomenon. Many investigations have been made concerning the mechanisms of cracking [1–4]. The susceptibility of carbon steels is frequently found to be limited to the active–passive region of potentials. The presence of the oxide film, its nature and the level of electrode potential have an important influence on caustic embrittlement [5, 6]. In the passive region, some data have indicated that anodic protection ensured the complete prevention of caustic embrittlement of welded mild steel equipment in the aluminium industry in Germany [7] and in the pulp and paper industry in Canada [8].

Iron passivity has been studied thoroughly in neutral or near-neutral electrolytes, while for alkaline solutions little research has been published [9–12]. Moreover, unanimous agreement on the mechanism and kinetics of film growth, the structure and properties of the passive film, and the effects of environmental factors (electrolyte, temperature, pressure, etc.) has not been achieved. The objectives of this work are to investigate the electrochemical behavior as related to the embrittlement of A516 pressure vessel steel (ASTM) in caustic aluminate or Bayer solutions, as used for the dissolution of bauxite, at different temperatures.

The effect of impurities such as AlO_2^-, CO_3^{2-}, SO_4^{2-} and other organic material contained in industrial Bayer solutions was studied as a function of temperature and potentials. The activation energy and the corrosion rates were evaluated for the critical and passive states. Stress corrosion cracking experiments were conducted with an MTS machine at a slow strain rate $2.6 \times 10^{-6}\,s^{-1}$ to verify the embrittlement of A516 steel in these two regions and the efficiency of anodic protection. At the same time, the electrochemical behavior was investigated by potentiodynamic and potentiostatic studies combined with surface analysis by SEM and EDAX for identifying the passive film.

2. Experimental details

2.1. *Materials*

Experiments were conducted on ASTM A516 grade 70 carbon steel (pressure vessel quality) with chemical composition presented in Table 1. The steel plates were cut to give cylindrical working electrodes of 0.32 cm^2 for electrochemical studies, or smooth tensile specimens of 25.4 mm gage length and 4 mm diameter for slow strain rate corrosion studies. Before each experiment, the electrodes were polished with emery paper from grit 240 to 600, rinsed with distilled water, diluted HCl (10%) and finally distilled water. Before starting the test, the electrodes were polarized cathodically at -1.1 V vs NHE for 5 min.

2.2. *Electrolytes*

Three electrolytes were used: 2.25 M NaOH, 3.6 M NaOH + 0.67 M $Al_2O_3 \cdot 3H_2O$ and Bayer solution containing 3.6 M NaOH, 0.67 M $Al_2O_3 \cdot 3H_2O$, 0.46 M Na_2CO_3, 0.02 M Na_2SO_4 and some organic carbon impurities.

0021-891X/89 $03.00 + .12

Table 1. Chemical compostion of A516 steel (wt%)

C	Mn	P	S	Si	Cu	Ni	Cr	Mo	Sr	Fe
0.24	1.15	0.008	0.007	0.25	0.044	0.025	0.033	0.004	0.002	balance

All these solutions had the same quantity of free NaOH (2.25 M) since the last two electrolytes contain a part of the total NaOH in a combined form with Al_2O_3 according to:

$$2NaOH + Al_2O_3 \cdot 3H_3O \longrightarrow 2NaAlO_2 + 4H_2O$$

The solutions were heated and maintained at 30, 65 and 100° C by an oil-thermostated bath. They were deaerated by prepurified argon before and during the experiment. Some preliminary studies showed that saturation of the solution by atmospheric oxygen did not sensibly affect the stress corrosion phenomenon.

2.3. *Experiments*

Slow strain rate experiments were conducted with an MTS machine at a rate of $2.6 \times 10^{-6}\ s^{-1}$ which leads to severe cracking [5]. A critical anodic potential in the SCC region was imposed during the test by means of a potentiostat.

Electrochemical experiments were carried out in a two-compartment cell made of Teflon. A conventional system composed of a potentiostat (PAR model 173, 376), a programmer (Par model 175), an *X–Y* recorder (Hewlett–Packard model 2D-2) and a high speed electronic recorder (Hewlett–Packard model 709A) were used for this purpose. Electrode potentials were measured with respect to a saturated calomel electrode (SCE) and converted to the normal hydrogen electrode scale (NHE)

The overpotential due to the thermal gradiant and uncompensated resistance between the working electrode and the Luggin probe have been neglected. These effects have been found to be significantly less than the error in the peak potential (≈ 30 mV) [11]. For obtaining reproducible results, the preparation and cleaning of the electrodes were carried out carefully. Triplicate tests were performed and reproducibility was found to be of the order of 90% for potential and current peaks. For slow strain rate tests, due to the length of the experiment, only two tests were completed for each set of parameters and reproducibility was $\pm 5\%$.

The oxide films obtained at the critical and passive states were examined by SEM using a JEOL-2553 apparatus combined with EDAX analysis (Tracor Northern equipment).

Potentiodynamic studies were carried out by scanning at 10 and $0.17\ mV\ s^{-1}$ between -1.10 and $+0.79$ V vs NHE. For the corrosion behavior diagram (CBD) [13], a scan rate of $14\ mV\ s^{-1}$ was used for drawing the three composite polarization curves. The first scan from -1.10 to $+0.79$ V vs NHE gave the corrosion potential E_1, and in the reverse scan (second scan), the corrosion potential E_2 was observed. The potentiostat was then turned off for a period up to 1 h during which a spontaneous polarization and a relative steady state were reached (E_3). Steady state conditions were arbitrarily assumed in these experiments when the potential change was less than $1\ mV\ min^{-1}$. The third cathodic curve was drawn from the equilibrium corrosion potential, E_3.

3. Results and interpretations

3.1. *Slow strain rate (SSR) experiments*

The susceptibility of A516 steel to SCC in the three electrolytes studied in two regions of the anodic polarization curve was evaluated by SSR experiments. Critical potentials in the active–passive region, determined by the transient method [5], and a potential in the passive range (-8 mV vs NHE) were retained for simulating the conditions of embrittlement and anodic protection, respectively. The susceptibility to cracking was estimated by the reduction of area (ROA). An experiment in oil at 100° C, where no corrosion is supposed to occur, was used as reference. The results are given in Table 2.

In the active–passive potential range, A516 steel is susceptible to caustic embrittlement. AlO_2^- ions and other impurities of Bayer solution promote more severe cracking than in pure NaOH solution. The influence of aluminate ions AlO_2^- is about three times that of all other impurities in Bayer solution. At the potential in the passive range (-8 mV vs NHE), the percentage of ROA is similar to that obtained in oil at the same temperature for the pure caustic solution, while in caustic aluminate and in Bayer solution, a certain embrittlement is noted, which is more evident for the latter environment.

The susceptibility to cracking was also verified by the presence of secondary cracks on the gage length by

Table 2. Susceptibility of A516 steel to SCC in hot caustic and caustic aluminate solutions (100° C). E_{crit} and $E = -8$ mV vs NHE are imposed potentials

Electrolytes	$E_{imposed}$ *(mV vs NHE)*	$ROA/ROA_{(oil)}$*
2.25 M NaOH	−683	0.90
	−8	0.97
3.6 M NaOH + 0.67 M Al_2O_3	−708	0.77
	−8	0.95
Bayer	−708	0.73
	−8	0.91

* $ROA_{(oil)} = 0.583$.

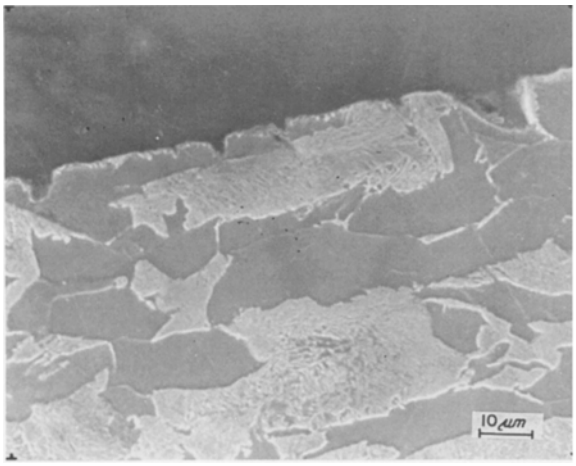

Fig. 1. Secondary intergranular cracks observed on the gage length of A516 steel in 2.25 M NaOH at 100° C. $E_{imposed} = -925$ mV vs SCE (or -683 mV vs NHE).

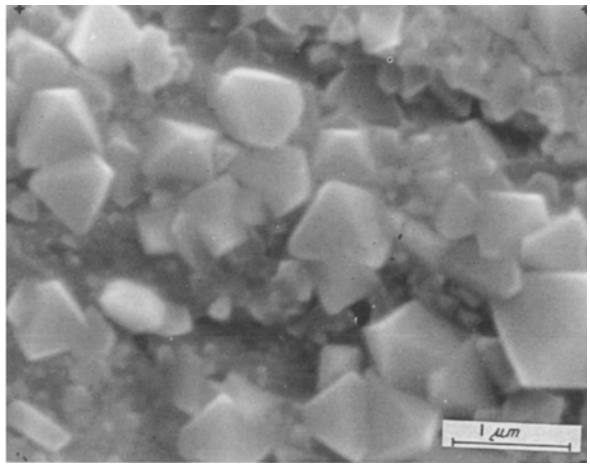

Fig. 2. View of the oxide film formed in the active–passive region in 2.25 M NaOH at 100° C. $E = -708$ mV vs NHE.

SEM. At the critical potentials situated in the active–passive range, intergranular and parallel cracks were observed on all the specimens (Fig. 1). The cracks were deeper in caustic aluminate and Bayer solutions than in pure NaOH electrolyte. At the passive potential (-8 mV vs NHE), in 2.25 M NaOH, no cracks were detected indicating the absence of SCC, while in the presence of AlO_2^- ions or other impurities, some cracks were initiated and propagated so slowly that shallow pits were formed.

3.2. *SEM studies on the oxide films*

The oxide films produced on the electrode surface after potentiodynamic, potentiostatic and galvanostatic experiments in three studied solutions at 100° C were observed by SEM and analyzed by EDAX.

Close to the transpassive zone (+792 mV vs NHE) of the potentiodynamic scan in 2.25 M NaOH solution, or after a galvanostatic experiment with an imposed anodic current 1 mA cm^{-2} for 5 min, the film consisted of well-defined crystallites on a base layer with different apparent structure. It was similar to that reported by other researchers by potentiostatic or galvanostatic experiments. The upper layer is composed of crystallites with highly developed crystallographic faces. Cubic crystallites indicate the probable presence of Fe_3O_4 and hexagonal crystallites $Fe(OH)_2$. The electrode is covered by a base gelatinous layer consisting of hydrated FeOOH or $Fe_2O_3 \cdot nH_2O$ [14, 15].

The micrograph of A516 steel, polarized from -1098 to -708 mV vs NHE (active–passive region) in 2.25 M NaOH shows large crystallites which present the most common crystal feature of Fe_3O_4 (Fig. 2). Moreover, the oxide is black and magnetic and analysis by X-ray diffraction technique confirmed the presence of Fe_3O_4. At -8 mV vs NHE (passive region), the film seems more compact and the crystallites are in a cubic or tabular form indicating the possible presence of Fe_2O_3. This is confirmed by the reddish color and the non-magnetic property of this oxide.

The oxide film, obtained by potentiostatic experiments by jumping from -1.1 V vs NHE to -708 or -8 mV vs NHE, is not as thick as that obtained previously by potentiodynamic scan, and the crystallites are not clearly developed. The same observations are valid for caustic aluminate or Bayer solutions. In addition, when AlO_2^- ions are present in the electrolytes, elongated crystallites are observed on the electrode surface. The EDAX analysis of the oxide film revealed the presence of Al species. In Bayer solutions, the oxide film formed on the electrode surface appears very thin and the observation by scanning electron microscope did not show a well-defined structure. The EDAX analysis indicated a greater quantity of Al in the oxide film.

3.3. *Potentiodynamic studies*

Employing the approach suggested by Parkins [2] for determining the susceptibility of steel to SCC, potentiodynamic curves were drawn at 0.17 and 10 mV s^{-1}. The occurrence of SCC implies a balance between active and passive behavior for initiating and retaining the geometry of the crack. Our results showed that the active–passive region is localized from about -0.758 to -0.600 V vs NHE. Typical potentiodynamic curves drawn at 30 and 100° C are presented in Fig. 3.

At 30° C, in the three studied solutions, two anodic peaks are observed on the i–E profile, recorded with the slow sweep rate 0.17 mV s^{-1}, and they are noted as peak II and peak III. They are well defined in pure caustic solution (2.25 M NaOH) but in the two other electrolytes these anodic peaks become larger and less sharp than in the plain caustic solution. At the top of the passive region, before oxygen evolution, the passive current densities remain almost the same for the three solutions. With the fast potential sweep rate 10 mV s^{-1}, the anodic peaks are not resolved as clearly as with the slow scan rate, especially in 2.25 M NaOH solution. An increase of anodic activity in the potential region of peak II is even observed in caustic aluminate solution. In the presence of the impurities

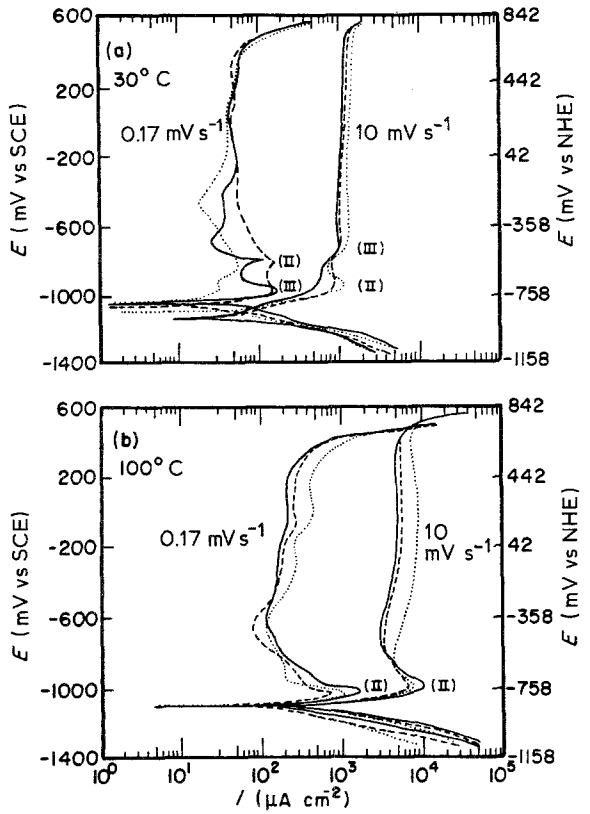

Fig. 3. Polarization curves of A516 steel in different solutions: —— 2.25 M NaOH; – – – 3.60 M NaOH + 0.67 M Al_2O_3; ···· Bayer. (a) 30° C; (b) 100° C.

of the Bayer solution, anodic peak II is more clearly observable on the curve and the current density of this peak is more than 5 times that obtained in 2.25 M NaOH. It should be noted that, in the three studied solutions, a real passivation is not observed with the fast scan rate.

At high temperature, 100° C, for both scan rates 0.17 and 10 mV s^{-1}, the anodic peak II is well defined and the passive region is located between −0.510 and 0.750 V vs NHE. Raising the temperature from 30 to 100° C increases the critical current density prior to passivation (peak II) more than one decade in 2.25 M NaOH and a little less in the two other solutions. At the same time, peak III decreases and remains a trace on the polarization curve. It appears as a shoulder of peak II especially at the slow scan rate, or is completely overlapped by peak II and the passive current as in the Bayer solution. The influence of AlO_2^- ions on the anodic dissolution of peak II is particularly observed at 100° C: the inhibition is about 40%. The current peak II decreases from 10 mA cm^{-2} in 2.25 M NaOH to 6 mA cm^{-2} in 3.6 M NaOH + 0.67 M Al_2O_3 in Bayer solution. The inhibition of dissolution at peak II is about 20% lower in Bayer solution than in caustic aluminate solution, due to the presence of impurities. Accompanying that effect, it is noted that the onset of passivity is slightly more active in caustic aluminate and Bayer solutions than in pure caustic solution. However, the influence of aluminate ions or impurities other than AlO_2^- is not the same as described earlier in the passive range. Instead of inhibiting corrosion, these impurities accelerate the metal dissolution. An increase of the passive current density (i_{pass}) is observed, especially in Bayer solution where i_{pass} is about 40% higher than i_{pass} in 2.25 M NaOH, while in 3.6 M NaOH + 0.67 M Al_2O_3, the increase of i_{pass} is only about 10%. This indicates that the 'passive' film, produced at the electrode surface in caustic aluminate and particularly Bayer solutions, is not as protective as that formed in NaOH solutions.

3.4. *Corrosion rate studies*

3.4.1. Free corrosion rates and passivation characteristics. The free corrosion current densities (i_{corr}) were determined from the polarization curves recorded at 0.17 mV s^{-1} by the anodic and cathodic Tafel plots. The calculation was performed by the EG&G (PAR) Model 332 Softcorr Corrosion Software and the results are given in Table 3. The anodic Tafel constant, β_a, was determined from a limited zone of $\approx$ 50 mV and the order of current magnitude ranged from 1 to 3 depending on the operating conditions. The cor-

Table 3. Free corrosion data of A516 steel in 2.25 M NaOH, 3.6 M NaOH + 0.67 M Al_2O_3 and Bayer solutions at different temperatures

Solution	*T (° C)*	*E_{corr} (mV vs NHE)*	*β_a (mV decade^{-1})*	*β_c (mV decade^{-1})*	*Corrosion rate (m s^{-1})**	*R_p (Ω m^2)*	*Corrosion rate (m s^{-1})***
2.25 M NaOH	30	−802	40	120	0.37×10^{-11}	0.165	0.29×10^{-11}
	65	−825	40	90	2.10×10^{-11}	0.019	2.32×10^{-11}
	85	−849	45	90	3.97×10^{-11}	0.012	4.01×10^{-11}
	100	−854	55	96	8.02×10^{-11}	0.008	6.99×10^{-11}
3.6 M NaOH + 0.67 M Al_2O_3	30	−839	ND	103	0.77×10^{-11}	0.071	0.74×10^{-11}
	65	−848	52	100	2.39×10^{-11}	0.023	2.39×10^{-11}
	85	−853	52	103	4.45×10^{-11}	0.014	3.94×10^{-11}
	100	−857	55	110	7.50×10^{-11}	0.008	7.32×10^{-11}
Bayer	30	−810	ND	155	2.39×10^{-11}	0.080	1.21×10^{-11}
	65	−833	ND	148	5.89×10^{-11}	0.018	5.11×10^{-11}
	85	−868	80	130	8.09×10^{-11}	0.011	7.21×10^{-11}
	100	−868	83	140	13.02×10^{-11}	0.006	13.90×10^{-11}

ND Not determined due to the fact that the anodic part is not sufficient for drawing the anodic Tafel plot.
i^*_{corr} Corrosion current density deduced from the anodic and cathodic Tafel plots.
i^{**}_{corr} Corrosion current density determined by the polarization resistance.

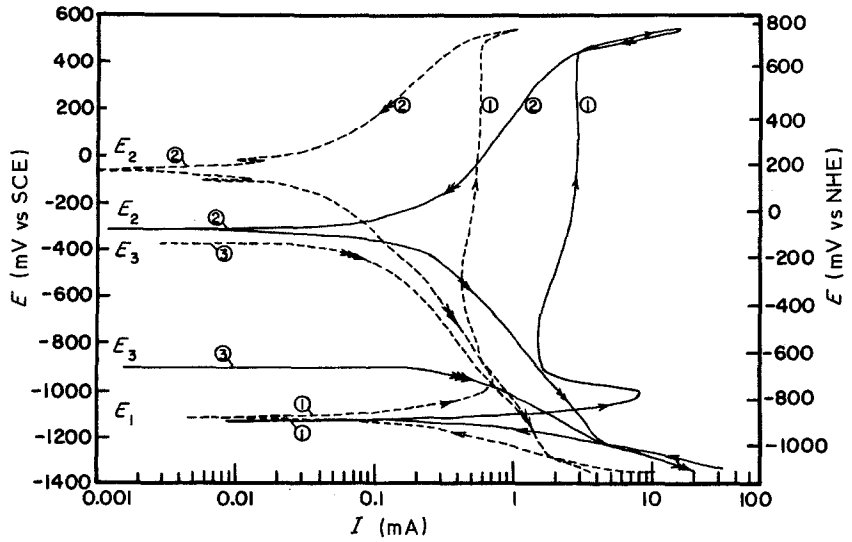

Fig. 4. Corrosion behavior diagram for A516 steel in Bayer solution at 30 (– – –) and 100°C (——). $dE/dt = 14\,mV\,s^{-1}$, electrode area = $0.72\,cm^2$. (1) First cathodic and anodic scans; (2) second cathodic and anodic scans; (3) third cathodic scan.

rosion current densities, determined by the Tafel method using anodic and cathodic polarization curves, coincide with those of the polarization resistance [16]. The corrosion rates increased, with increase in temperature and also with the presence of AlO_2^- ions or the impurities in the Bayer solution. A decrease of the polarization resistance R_p in such cases is observed and is in accordance with the increase of the corrosion rates.

The corrosion rates on a passive surface were calculated by using the corrosion behaviour diagram (CBD) as used by Inco company [13] and EG&G Princeton Applied Research Laboratory [17]. This method makes use of the rapid-scan potentiodynamic technique to produce a series of polarization curves that describe an alloy's corrosion characteristics in the test environment. The method has yielded calculated corrosion rates that correspond to rates obtained from conventional long-term immersion tests [17]. In the three studied solutions, high passive current densities were observed during the active-to-noble and reverse scans at all temperatures (Fig. 4). This indicates that the passivation of A516 steel is poor in these solutions and dissolution continues even in the passive state. Also, the oxide film, formed during the anodic polarization, is not readily reduced during the reverse scan, and this observation is illustrated by an important noble shift of the corrosion potential E_2 with respect to E_1 (Table 4). These are the two main differences between the passivation behavior of this system as compared to that of passive Ni–Cr–Mo alloys [13].

The temperature has a marked effect on the stability of the passive film such as indicated by the corrosion potentials E_2 and E_3. The corrosion potentials E_2 are more noble at low temperatures than at high temperatures while E_3 becomes more active with increase of temperature. This confirms the resistance of a passive film at low temperature; an increase in temperature facilitates the reduction of the oxide film at the electrode surface. The presence of the impurities of the Bayer solution, and especially AlO_2^- ions, gives a more active E_2 for all temperatures as compared to pure NaOH solutions. It should be noted that the impurities of the Bayer solution have a very marked effect on E_2,

Table 4. Corrosion rates of A516 steel evaluated by the CBD technique [13] on a passive surface electrode

Solution	*T (°C)*	*i_{corr} (CBD) ($A\,m^{-2}$)*	*Corrosion rates ($m\,s^{-1}$)*	*E_1 (mV vs NHE)*	*E_2 (mV vs NHE)*	*E_3 (mV vs NHE)*	*$\Delta E = E_2 - E_1$ (mV)*
2.25 M NaOH	30	1.1	4.04×10^{-11}	−808	+262	−80	1070
	65	3.2	21.77×10^{-11}	−803	+342	−50	1145
	85	6.6	24.52×10^{-11}	−828	+202	−210	1030
	100	41.7	153.39×10^{-11}	−818	+192	−860	1010
3.6 M NaOH + 0.67 M Al_2O_3	30	1.4	5.15×10^{-11}	−888	+192	−108	1080
	65	3.1	11.40×10^{-11}	−858	+182	−118	1040
	85	3.9	14.35×10^{-11}	−858	+132	−128	990
	100	9.0	33.11×10^{-11}	−858	+2	−328	860
Bayer	30	1.4	5.15×10^{-11}	−928	+192	−118	1120
	65	3.2	11.77×10^{-11}	−868	+282	−108	1140
	85	5.1	18.76×10^{-11}	−858	+192	−203	1050
	100	20.8	76.51×10^{-11}	−878	−78	−658	800

Table 5. Crack propagation rates (CPR) of A516 in 2.25 M NaOH, 3.6 M NaOH + 0.67 M Al_2O_3 and Bayer solutions calculated from different anodic current densities

	Electrolyte											
	2.25 M NaOH				*3.6 M NaOH + 0.67 M Al_2O_3*				*Bayer*			
	30° C	*65° C*	*85° C*	*100° C*	*30° C*	*65° C*	*85° C*	*100° C*	*30° C*	*65° C*	*85° C*	*100° C*
i_{crit} ($A\,m^{-2}$)	3*	20	47	101	6	25	43	75	8.7	33	56	82
CPR ($10^{-11}\,m\,s^{-1}$)	11.1	73.6	172.9	371.5	22.1	91.9	158.2	275.9	32.0	121.4	206.0	301.6
i_{eff} ($A\,m^{-2}$)	2.3*	17	39	69	5.3	20	40	69	7.3	27	46	74
CPR ($10^{-11}\,m\,s^{-1}$)	8.5	62.5	143.5	253.8	19.5	73.6	147.1	253.8	26.9	99.31	169.2	272.2
i_{pass} ($A\,m^{-2}$)	0.6	1.2	2.1	2.5	0.6	1.2	2.2	2.8	0.5	1.3	2.2	3.6
CPR ($10^{-11}\,m\,s^{-1}$)	2.2	4.41	7.72	9.2	2.2	4.41	8.09	10.3	1.8	4.8	8.09	13.2

* The values are deduced from extrapolation of the current densities measured at high temperatures, as the critical peak II is not well defined at 30° C.

particularly at 100° C. The larger difference, ΔE, between E_1 and E_2 in 2.25 M NaOH than that obtained in the two other solutions at 100° C is in accordance with that observation.

It seems that the influence of the impurities on passivation is similar to the rise of temperature in this aspect. The corrosion potentials, E_3, are observed to be more noble in Bayer and especially in caustic aluminate solutions at 100° C than in pure caustic solution. Hence, in these conditions it appears that the electrode polarization is easier when impurities such as AlO_2^- ions are dissolved in the electrolyte at elevated temperatures. The polarization effects of these impurities are not important at temperatures below 65° C.

Concerning the corrosion rates, it is observed that they are higher at elevated temperatures as compared with low ones and that this tendency is consistent for the three studied solutions. At high temperatures, where susceptibility to caustic embrittlement is observed, the corrosion rates in the caustic aluminate and Bayer solutions are much lower than those in pure NaOH solutions, reflecting the facility of reduction of the passive film. Moreover, these results indicate that the nature of the passive film is varied from one solution to another. The impurities of Bayer solution must be incorporated in the passive film, especially AlO_2^- ions, and this is reflected by its lower current of reduction in these cases.

3.4.2. Crack propagation rates in the active and passive ranges. Several mechanisms for caustic cracking proposed a crack advancement by localized anodic dissolution at the tip in the presence of a film covering the crack surface. For estimating propagation rates of SCC, anodic current densities are measured on a bare surface [2, 4, 18] and converted to the corrosion rate. In considering the influence of the film formation of the crack tip, Parkins [2] estimated that the effective current density (i_{eff}) is the largest difference between fast and slow sweep rate polarization curves in the cracking potential region.

The corrosion rates calculated from the critical current density (i_{crit}) must be overestimated since the effect of the passive film was not considered. They were about 10–30% higher than those obtained from the approach of Parkins by considering i_{eff} (Table 5). With i_{eff}, the influence of Bayer solution impurities, including aluminate ions, on the susceptibility to SCC was verified. The increase of the crack propagation rates was observed for Bayer solution at all temperatures and for caustic aluminate at temperatures below 85° C.

In the passive region, the current density (i_{pass}), obtained at −8 mV vs NHE in our polarization curves recorded with the slow scan rate $0.17\,mV\,s^{-1}$, was used for calculating crack propagation rates. This potential was chosen because the passivity of the steel is attained at this potential range where anodic protection is usually considered. The applied anodic potential was far enough from the dangerous active–passive cracking region. An important increase of the propagation rates in Bayer solution was observed in comparison to pure caustic and caustic aluminate electrolytes. The crack propagation rates calculated with i_{pass} were in accordance with the slow strain rate results.

3.5. *Activation energy*

Tables 4 and 5 shows the corrosion rates are dependent on the temperatures, the presence of AlO_2^- ions and other impurities in the solution. The current densities also vary with the equilibrium, active or passive states. Arrhenius plots for these different states are considered (Fig. 5). A linear dependency is obtained in each case:

$$\log i = A - (B \times 1/T)$$

This equation is similar to the well-known Arrhenius relation:

$$\log i = A - (\Delta G/2.303RT)$$

where ΔG is the activation energy ($J\,mol^{-1}$); R is the gas constant ($8.314\,J\,K^{-1}\,mol^{-1}$); and A and B are constants.

The values of $\Delta G/2.303R$ can be derived from the slope of the $\log i$ vs $1/T$ plot and the activation energy,

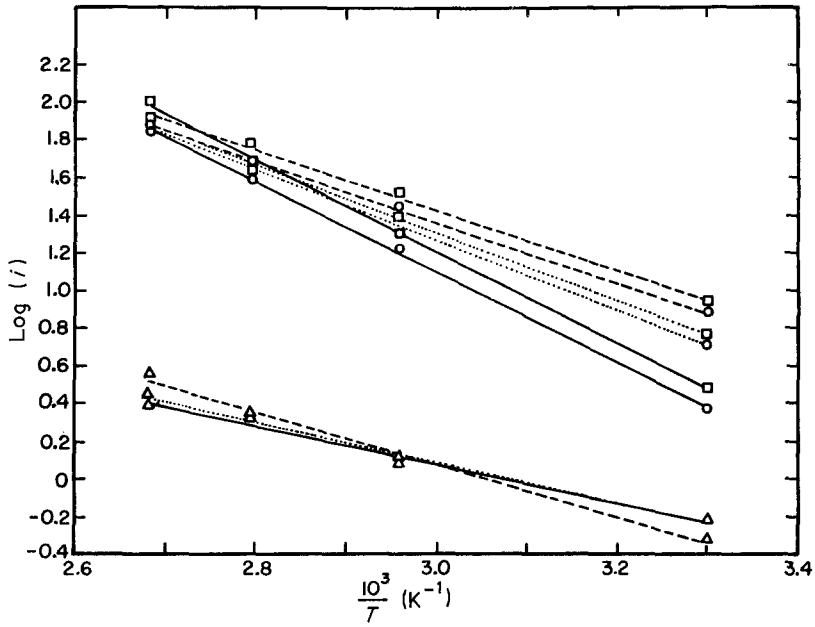

Fig. 5. Log i vs $1/T$ plot of A516 steel in 2.25 M NaOH (——), 3.6 M NaOH + 0.67 M Al_2O_3 (· · ·) and Bayer (– – –) solutions. □, Critical state; ○, active–passive state; △, passive state.

ΔG can be deduced by computing the values of log i and $1/T$ and calculating ΔG by linear regression. The results are presented in Table 6.

It is observed that for all the states, except for the passive state, AlO_2^- ions and Bayer solution impurities lower the activation energy. The values of ΔG corresponding to the critical state refer to the activation energy necessary for the anodic process of passive film formation. In caustic aluminate and Bayer solutions, a lower ΔG indicates that the passivation of steel is easier in these electrolytes than in 2.25 M NaOH. The inhibition effect is particularly important in caustic aluminate solutions. The presence of AlO_2^- ions in solution reduces the activation energy for passive film formation by about 28% while the impurities other than AlO_2^- in the Bayer solution contribute only to about a 7% reduction of ΔG.

In the passive state, an inverse situation is observed. Instead of reducing ΔG, AlO_2^- ions and Bayer solution impurities contribute to an increase in this quantity. The activation energy in the passive range refers to the energy of the anodic process for maintaining the passive film produced on the electrode surface. A lower activation energy indicates that the electrode is more readily kept in the passive state, and so a high value of ΔG can be interpreted as less stable passivation. An increase in ΔG is observed in caustic aluminate and Bayer solutions in comparison with the 2.25 M NaOH solution. The activation energy increases by about 5 and 30% in 3.6 M NaOH + 0.67 M Al_2O_3 and Bayer solutions respectively. The results agree well with the observed passive current density of A516 steel in these media.

4. Discussion

It is recognized that the slow strain rate technique leads to an extremely severe test for SCC in a short time. The results show that caustic embrittlement is detected when the specimen is polarized at a potential lying in the active–passive zone, especially at temperatures higher than 65° C. This critical temperature corresponds with that generally found in industry [18].

Thomas and Nurse [19] established a linear dependence of critical potentials on pH, for pH between 6 and 12:

$$E = 0.09 - 0.06\,\mathrm{pH} \quad (\mathrm{V\ vs\ NHE})$$

Table 6. Activation energy (ΔG) for the corrosion of A516 steel at equilibrium, critical, active–passive and passive states

Solution	$\Delta G\,(kJ\,mol^{-1})$			
	$E_{corrosion}$ (1)	$E_{critical}$ (2)	$E_{active\text{-}passive}$ (3)	$E_{passive}$ (4)
2.25 M NaOH	42.03 ± 1.82	46.53 ± 1.23	45.08 ± 1.26	19.70 ± 1.55
3.6 M NaOH + 0.67 M Al_2O_3	30.06 ± 1.44	33.32 ± 1.17	34.08 ± 0.94	20.79 ± 1.67
Bayer	21.89 ± 1.63	30.52 ± 1.15	30.77 ± 0.75	25.91 ± 1.15

(1) At $E_{corrosion}$, i_{corr} are used for calculating the corrosion rates (Equation 4).
(2) At $E_{critical}$, i_{crit} are used.
(3) At $E_{active\text{-}passive}$, i_{eff} are used.
(4) At $E_{passive}$, i_{pass} are used.

In our conditions the pH is more basic, about 13.8, and this relationship between E and pH is observed. The measured or calculated critical potentials are nearly the same, i.e., -738 V vs NHE in 2.25 M NaOH solution. In Bayer or caustic aluminate solutions, the critical potentials are shifted to 25 mV more active than in pure caustic solution. The susceptibility to cracking also increases with the presence of Bayer solution impurities, especially with the dissolved aluminate ions.

In the passive region the steel is protected against cracking in 2.25 M NaOH, but the presence of dissolved AlO_2^- ions or other impurities involve some embrittlement (Table 2). This is particularly interesting for the application of anodic protection recently installed on some process vessels in the alumina industry of Canada [20]. It shows that the polarization in the passive zone is beneficial but does not completely protect the industrial equipment against SCC.

In pure caustic solution, cracking occurs probably in the presence of an Fe_3O_4 film formed from $Fe(OH)_2$ in the active–passive zone, while in the passive range, a layer of Fe_2O_3 is produced. This is in good agreement with Parkins [2], who suggested that cracking in hydroxide solutions occurs in the presence of Fe_3O_4 but not in the presence of Fe_2O_3. While aluminate ions are present in the electrolytes, our EDAX analysis confirmed an incorporation of Al in the oxide film to yield the formation of an amorphous film $Fe_{3-x}Al_xO_4 (x \leqslant 2)$, as suggested by Tromans *et al.* [21]. Aluminate ions facilitate the formation of the passive film. A possible explanation is that there is a competitive adsorption between OH^- and AlO_2^- at the electrode surface that results in a decrease of concentration of $FeOH_{ads}$ species and that this retards the active dissolution of iron via the reaction

$$FeOH_{ads} + H_2O \longrightarrow HFeO_2^- + 3H^+ + 2e$$

The formation of a passive film containing aluminate ions increased the susceptibility to SCC. In Bayer solution, the inhibiting effect of impurities other than AlO_2^- is less important. All the impurities in the Bayer solution must limit the mass transport of dissolved AlO_2^- anions to the surface and decrease the concentration of $FeAlO_2^-$ species. This may have direct consequences on the inhibiting effect in this solution.

However, in the passive region, the presence of these impurities greatly affects the stability and the morphology of the passive film. It seems that defects in the oxide film are more numerous in Bayer solution than in pure caustic electrolyte [22]. These defects can be the points for initiation and propagation of cracks. Embrittlement observed in the passive range in Bayer and caustic aluminate solutions agrees with this hypothesis.

The CBD technique is very useful for studying passivity of the steel in relation to the investigation of the SCC susceptibility in these electrolytes. Passivation is easy but the oxide film is not stable when the temperature is increased or the Bayer solution impurities, including AlO_2^-, are present in the solutions.

Finally, it appears reasonable to believe that the controlling process in stress corrosion cracking of A516 steel in these studied solutions is crack tip dissolution. The activation energy for the crack propagation rates calculated with i_{eff} is almost the same to that for intense anodic dissolution on a relatively bare surface deduced from i_{crit}. In sodium hydroxide solution, an activation energy of 46 kJ mol^{-1} is slightly higher than the activation energy of about 42 kJ mol^{-1} in 1 N Na_2CO_3 + 1 N $NaHCO_3$ obtained by Parkins [2]. Aluminate ions and other impurities dissolved in solutions lower the activation energy to about 30–34 kJ mol^{-1}.

5. Conclusions

(1) Stress corrosion cracking is more important in caustic aluminate and Bayer solutions than in pure 2.25 M NaOH. SCC cannot be completely prevented by anodic protection in the aluminate containing solutions.

(2) SEM studies of the oxide film in 2.25 M NaOH at 100° C reveal the formation of a probable Fe_3O_4 layer in the active–passive transition zone and Fe_2O_3 in the passive region. When AlO_2^- ions are present in the electrolyte, formation of an amorphous $Fe_{3-x}Al_xO_4$ ($x \leqslant 2$) film is expected.

(3) Bayer solution impurities, and especially AlO_2^- ions, facilitate the passivation but the passive film is not as stable as in pure NaOH. Anodic polarization curves and, especially, the CBD technique are very helpful for determining these characteristics of the passive film.

(4) Crack propagation rates increase with the presence of Bayer solution impurities, including AlO_2^- ions, as indicated by the values of activation energy. The controlling process in SCC of A516 must be dissolution at the crack tip. The activation energy is about 46 kJ mol^{-1} in 2.25 M NaOH and it decreases to 34 and 30 kJ mol^{-1} in 3.6 M NaOH + 0.67 M Al_2O_3 and Bayer solution, respectively.

Acknowledgement

The authors are thankful to the National Science and Engineering Research Council of Canada (NSERC) for providing financial support.

References

[1] H. L. Logan, *J. Res. Nat. Bur. Stand.* **48** (1952) 99.
[2] R. N. Parkins, *Corros. Sci.* **20** (1980) 147.
[3] J. C. Scully, *Corros. Sci.* **15** (1975) 207.
[4] T. P. Hoar and R. W. Jones, *Corros. Sci.* **13** (1973).
[5] A. Wieckowski, E. Ghali and H. H. Le, *J. Electrochem. Soc.* **131** (1984) 2024.
[6] E. Ghali, A. Wieckowski and H. H. Le, Proc. 9th Int. Cong. Metallic Corrosion, NACE (1984) Vol. 2. p. 195.
[7] H. Grafen, *Werkst. Korros.* **20** (1969) 305.
[8] W. A. Mueller, Pulp Paper Ind. Corros. Probl. (Int. Semin), 1st, 2nd NACE, Houston, Texas, (1977) p. 140.
[9] Z. Szklarska-Smialowska and W. Kozlowski, *J. Electrochem. Soc.* **131** (1984) 234.
[10] D. D. MacDonald and B. Roberts, *Electrochim. Acta* **23** (1978) 557, 781.

[11] A. Wieckowski and E. Ghali, *Electrochim. Acta* **30** (1985) 1423.
[12] R. D. Armstrong and I. Bauhroo, *J. Electroanal. Chem.* **40** (1972) 325.
[13] P. E. Morris and R. C. Scarberry, *Corrosion* **28** (1972) 444.
[14] L. Ojefors, *J. Electrochem. Soc.* **123** (1976) 1691.
[15] D. D. MacDonald and D. Owen, *J. Electrochem. Soc.* **120**, 3 (1973) 317.
[16] M. Stern and A. L. Geary, *J. Electrochem. Soc.* **104** (1957) 56.
[17] EG&G. Parc., Application notes Corr-1 (1982).
[18] G. Fulford, Review of Data on Caustic Cracking of Mild Steel. Alcan Research Laboratories, Kingston, Ontario, Canada (1982).
[19] J. G. N. Thomas and T. J. Nurse, *Br. Corros. J.* **2** (1967) 13.
[20] G. Riedl, Anodic Proctection. Internal report, Alcan Int. Ltée (1983).
[21] R. Siram and D. Tromans, *Corros. Sci.* **25** (1985) 79.
[22] H. H. Le and E. Ghali, to be published.